Adaptive Exploration for Data-Efficient General Value Function Evaluations

Arushi Jain
arushi.jain@mail.mcgill.ca
McGill University
Mila

Josiah P. Hanna
jphanna@cs.wisc.edu
The University of Wisconsin – Madison

Doina Precup
dprecup@cs.mcgill.ca
McGill University
Mila

Abstract

General Value Functions (GVFs) (Sutton et al., 2011) represent predictive knowledge in reinforcement learning. Each GVF computes the expected return for a given policy, based on a unique reward. Existing methods relying on fixed behavior policies or pre-collected data often face data efficiency issues when learning multiple GVFs in parallel using off-policy methods. To address this, we introduce `GVFExplorer`, which adaptively learns a single behavior policy that efficiently collects data for evaluating multiple GVFs in parallel. Our method optimizes the behavior policy by minimizing the total variance in return across GVFs, thereby reducing the required environmental interactions We use an existing temporal-difference-style variance estimator to approximate the return variance. We prove that each behavior policy update decreases the overall mean squared error in GVF predictions. We empirically show our method's performance in tabular and nonlinear function approximation settings, including Mujoco environments, with stationary and non-stationary reward signals, optimizing data usage and reducing prediction errors across multiple GVFs.

1 Introduction

The ability to make multiple predictions is a key attribute of human, animal, and artificial intelligence. Sutton et al. (2011) introduced **General Value Functions (GVFs)** which consists of several independent sub-agents, each responsible for answering specific predictive knowledge about the environment. Each GVF consists of a unique - policy, custom reward function called *cumulant* and state-dependent discount factor - to calculate the cumulative discounted cumulant. For example, a GVF can predict the expected number of times an agent will bump into the wall under a given policy (White et al., 2015; Schlegel et al., 2021; Sherstan, 2020). In essence, GVFs generalizes the standard value function to address a wider range of predictive questions, making them a powerful tool for intelligent systems.

Prior works have used either a fixed randomized behavior policy (Sutton et al., 2011) or pre-collected datasets (Xu et al., 2022) to update all GVFs in parallel using *off-policy learning*. However, these methods can result in large value estimation errors if the behavior policy significantly diverges from the GVF policies. Our work addresses this gap by focusing on the question of exploration for evaluating GVFs: *how can we adapt an agent's behavior policy to data-efficiently sample for evaluating multiple GVFs in parallel?* While exploration has been extensively studied in context of optimal control in Markov Decision Processes (MDP), the question of constructing a policy that can learn multiple quantities in parallel has remained largely untouched.

To accurately evaluate multiple GVFs in parallel, we aim to design a behavior policy that minimizes the overall *mean squared error (MSE)* in their predictions. A natural approach might involve following each GVF's target policy for some period of time (e.g. one episode) in a round-robin manner while concurrently updating all GVFs off-policy. However, this approach can be highly data inefficient as

17th European Workshop on Reinforcement Learning (EWRL 2024).

actions are sampled according to given policies, potentially overlooking actions from states where expected return is uncertain. To achieve better value estimation in fewer samples, it is essential to focus on state-action pairs with high variance in return, as these pairs would exhibit greater uncertainty in their mean return. Therefore, a behavior policy should visit such pairs more frequently to offset higher variance in return. Consider an analogy of two-arm bandit problem: fewer samples are needed for a constant reward arm for accurate value estimation, whereas an arm with a variable reward demands a greater number of samples to achieve the same level of certainty. We empirically support this claim by comparing round-robin and our proposed approach later.

With this motivation, we introduce `GVFExplorer`, that adaptively learns a behavior policy which minimize the total MSE across all GVF predictions. `GVFExplorer` leverages the existing off-policy temporal difference (TD) based estimator of variance in return distribution (Sherstan et al., 2018; Jain et al., 2021) to guide the behavior policy. The strategy is to frequently take actions that might have more unpredictable outcomes (high variance in return). By sampling them more, agent can estimate the mean return better with fewer interactions, thus effectively lowering the overall MSE in the GVF predictions.

`GVFExplorer` optimizes the data usage and reduces the prediction error, offering a scalable solution for complex environments. This is particularly valuable for real-world applications like personalized recommender systems (Parapar & Radlinski, 2021; Tang et al., 2015), where it can enable efficient evaluation of personalized policies based on diverse user preferences (reward functions) (Li et al., 2024), leveraging shared knowledge for improved accuracy.

Contributions: (1)We design an adaptive behavior policy that enables accurate and efficient learning of multiple GVF predictions in parallel [Algorithm 1]. (2) We derive an iterative behavior update rule that directly minimizes the overall prediction error [Theorem 4.1]. (3) We prove in tabular setting that each iterative update to the behavior policy causes the total MSE across GVFs to be less than equal to one from the old policy [Theorem 4.2]. (4) We establish the existence of a variance operator that enables us to use TD-based variance estimation [Lemma 5.1]. (5) We empirically demonstrate in both tabular and Mujoco environments that `GVFExplorer` lowers the total MSE when estimating multiple GVFs compared to baseline approaches and enables evaluating a larger number of GVFs in parallel.

2 Related Work

Exploration in reinforcement learning (RL) has predominantly focused on improving policy performance for a single objective (Oudeyer et al., 2007; Schmidhuber, 2010; Jaderberg et al., 2016; Machado et al., 2017; Eysenbach et al., 2018; Burda et al., 2018; Guo et al., 2022). Refer to Ladosz et al. (2022) for a detailed survey on exploration techniques in RL. While related to exploration, these works differ from ours, as they concentrate on optimizing policies for single objective rather than evaluating multiple GVFs (policy-cumulant pair) simultaneously.

Our work is most closely related to other works on learning multiple GVFs. Xu et al. (2022) address a similar problem by evaluating multiple GVFs using an offline dataset, but our method operates online, avoiding the data coverage limitations of offline approaches. Linke et al. (2020) develops exploration strategies for GVFs in a stateless bandit context, which does not deal with the off-policy learning or function approximation challenges present in the full Markov Decision Process (MDP) context. In a single bandit problem, Antos et al. (2008); Carpentier et al. (2015), show that the optimal data collection strategy to estimate mean rewards of arms is to sample proportional to each arm's variance in reward. Prior works like Hanna et al. (2017) learned a behavior policy for a *single* policy evaluation problem using a REINFORCE-style (Williams, 1992) variance-based method called `BPS`. This idea extends on the similar principles of using Importance Sampling in Monte Carlo simulations for finding optimal sampling policy based on variance minimization (Owen, 2013; Frank et al., 2008). Metelli et al. (2023) extends this idea to the control setting. However, these methods are limited to single-task evaluation or control. Evaluating multiple policies simultaneously is more complex, requiring careful balance in action selection among interrelated learning problems. Perhaps the closest work to ours is by McLeod et al. (2021), which uses the changes in the weights of Successor Representation (SR) (Dayan, 1993) as an intrinsic reward to learn a behavior policy that supports multiple predictive tasks. `GVFExplorer` approach is simpler, as it directly optimizes the behavior

policy to minimize the total prediction error over GVFs, resulting in an intuitive variance-proportional sampling algorithm. We will compare the two approaches empirically as well.

3 Preliminaries

Consider an agent interacting with the environment to obtain estimates of $\mathcal{N}$ different *General Value Function* (GVF) (Sutton et al., 2011). We assume an episodic, discounted Markov decision process (MDP) where $\mathcal{S}$ is the set of states, $\mathcal{A}$ is the action set, $\mathcal{P} : \mathcal{S} \times \mathcal{A} \to \Delta_{\mathcal{S}}$ is the transition probability function, $\Delta_{\mathcal{S}}$ is the $|\mathcal{S}|$-dimensional probability simplex, and $\gamma \in [0, 1)$ is the discount factor.

Each GVF is conditioned on a fixed policy $\pi_i : \mathcal{S} \to \Delta_{\mathcal{A}}$, $i = \{1, \ldots, \mathcal{N}\}$ and has a cumulant $c_i : \mathcal{S} \times \mathcal{A} \to \mathbb{R}$. For simplicity, we assume that all cumulants are scalar, and that the GVFs share the environment discount factor γ. This eases the exposition, but our results can be extended to general multidimensional cumulants and state dependent discount factor. Each GVF is a value function $V_{\pi_i}(s) = \mathbb{E}_{\pi_i,\mathcal{P}}[G^i_t | s_t = s]$ where $G^i_t = c_{i,t} + \gamma G^i_{t+1}$. Each GVF can be viewed as answering the question, "what is the expected discounted sum of c_i received while following π_i?" We can also define action-value GVFs: $Q_{\pi_i}(s, a) = c_i(s, a) + \gamma \mathbb{E}_{s' \sim \mathcal{P}(\cdot|s,a)}[V_{\pi_i}(s')]$, with $V_{\pi_i}(s) = \mathbb{E}_{a \sim \pi_i(\cdot|s)}[Q_{\pi_i}(s, a)]$.

At each time step t, the agent in state s_t, takes an action a_t and receives cumulant values $c_{i,t}$ for all $i \in \{1, \ldots, \mathcal{N}\}$, transitioning to a new state s_{t+1}. This repeats until reaching a terminal state or a maximum step count. Then the agent resets to a new initial state and starts again. The agent interacts with environment using a behavior policy, $\mu : \mathcal{S} \to \Delta_{\mathcal{A}}$. The goal is to approximate values $\hat{V}_i$ corresponding to the true GVFs value V_{π_i}. We formalize the objective as **minimizing the Mean Squared Error (MSE)** under some state weighting $d(s)$ for all GVFs:

$$MSE(V, \hat{V}) = \sum_{i=1}^{\mathcal{N}} \sum_{s \in \mathcal{S}} d(s) \Big(V_{\pi_i}(s) - \hat{V}_i(s) \Big)^2. \tag{1}$$

In our experiments, we use the uniform distribution for $d(s)$. This objective can be generalized to prioritize certain GVFs using a weighted MSE.

Importance Sampling (IS). To estimate multiple GVFs with distinct target policies π_i in parallel, off-policy learning is essential. Importance sampling (IS) is one of the primary tools for off-policy value learning (Hesterberg, 1988; Precup, 2000; Rubinstein & Kroese, 2016), allowing estimation of value function under target policy π using samples from different behavior policy μ. In context of off-policy Temporal Difference (TD) learning (Sutton & Barto, 2018), IS ratio, $\rho_t = \frac{\pi(a_t|s_t)}{\mu(a_t|s_t)}$, is used to adjust the updates to ensure *unbiased value estimates*. The update rule is given as $\hat{Q}(s_t, a_t) = \hat{Q}(s_t, a_t) + \alpha \Big(c_t + \gamma \rho_{t+1} \hat{Q}(s_{t+1}, a_{t+1}) - \hat{Q}(s_t, a_t) \Big)$, where α is the learning rate. This update rule ensures that estimated value function $\hat{Q}$ converges to correct value Q_π under policy π, despite the samples being generated from a behavior policy μ.

4 Behavior Policy Optimization

As described in the previous section, the goal of the agent is to minimize the total mean squared error (MSE) across the given GVFs (Eq. (1)). Note that MSE = Variance + Bias^2. For the algorithm's derivation, we will use **unbiased** IS estimation for off-policy correction, which shifts the task of minimizing MSE to reducing the total variance across GVFs. *Thus, the core problem is to design a behavior policy that collects data to* ***minimize the variance in return*** *across GVFs and accurately estimate multiple GVF value functions*.

The problem of estimating a *single target policy's* value V_π is well studied in the literature. Kahn & Marshall (1953); Owen (2013) uses IS through *variance minimization* to find the optimal behavior policy μ^*. Owen (2013) also showed that μ^* can lead to improved performance by using off-policy value estimation over direct sampling from π, with the improvement directly related to the degree of variance reduction. However, their analytical solution of obtaining μ^* depends on an unknown quantity V_π, making it impractical. Nonetheless, the insight suggests that minimizing variance may also enhance performance in policy control for multiple GVF scenarios. In this work, however, we

focus solely on policy evaluation, laying the foundation for potential future extensions to policy control.

4.1 Objective Function

We propose `GVFExplorer` to address the above limitation and extend the problem to accurately estimate multiple GVF values. `GVFExplorer` takes as input the GVF target policies $\pi_{i=\{1,\dots,\mathcal{N}\}}$, uses off-policy algorithm to sample the data from behavior policy μ (which is optimized over time) and outputs the GVF estimates $\hat{V}_{i=\{1,\dots,\mathcal{N}\}}$. Since our objective is to find a behavior policy that minimizes the variance in return across multiple GVFs, we use existing off-policy TD-style variance estimator (Sherstan et al., 2018). This estimator allows to bootstrap the target values and iteratively update the variance function, making the solution scalable to complex domains.

We define the variance function by $\boldsymbol{M_{\pi}^{\mu}(s)}$, which measures the **variance in the return** of target policy π in a given state s when actions are sampled under a different behavior policy μ. In-depth insights into the variance operator is explored in Sec. 5. The variance function for a given state and a give state-action pair is defined respectively:

$$M_{\pi}^{\mu}(s) = \text{Var}_{\pi}(G_t|s_t = s, a \sim \mu) \quad \text{and} \quad M_{\pi}^{\mu}(s,a) = \text{Var}_{\pi}(G_t|s_t = s, a_t = a, a' \sim \mu).$$

Our objective is to find an optimal behavior policy μ^* that efficiently collects a single stream of experience to minimize the sum of variances $M_{\pi_{\{1\dots\mathcal{N}\}}}$ under some state distribution $d(s)$, as,

$$\mu^* = \arg\min_{\mu} \sum_{i=1}^{\mathcal{N}} \sum_{s} d(s) M_{\pi_i}^{\mu}(s) \quad \text{s.t.} \quad \mu(a|s) \geq 0 \,\&\, \sum_{a} \mu(a|s) = 1. \tag{2}$$

We solve the above objective function iteratively. At each iteration k, `GVFExplorer` produces a behavior policy μ_k. The behavior policy interacts with the environment and gathers data. Using this data, any off-policy TD algorithm can be used to iteratively estimate the variance function $M_{\pi}^{\mu_k}$. This variance function is used to update to a better policy μ_{k+1}, continuing the cycle similar to *policy iteration* in standard RL.

Our aim is to iteratively improve behavior policy and decrease variance functions to estimate the GVF values $V_{\pi_{i=\{1,2,\dots,\mathcal{N}\}}}$ with reducing MSE:

$$\mu_0 \xrightarrow{E} M_{\pi_{i=1,2,\dots}}^{\mu_0} \xrightarrow{I} \mu_1 \xrightarrow{E} M_{\pi_{i=1,2,\dots}}^{\mu_1} \dots \xrightarrow{E} \mu_K,$$

where $\xrightarrow{E}$ denotes *variance estimation* and $\xrightarrow{I}$ denotes *behavior policy improvement*. Next, we present Theorem 4.1 which principally derives the behavior policy update from μ_k to μ_{k+1} by solving the objective in Eq. (7). We demonstrate that the behavior policy update in Eq. (3) minimizes the objective by showing that μ_{k+1} is a better policy than μ_k. The policy μ_{k+1} is considered as good as, or better than μ_k, if it obtains lesser or equal total variance across all GVFs:$\sum_i M_{\pi_i}^{\mu_{k+1}} \leq \sum_i M_{\pi_i}^{\mu_k}$. The proof of behavior policy improvement is detailed in Theorem 4.2.

4.2 Theoretical Solution

Theorem 4.1. ***(Behavior Policy Update:)*** *Given $\mathcal{N}$ target policies π_i for $i \in \{1\dots\mathcal{N}\}$, let $k \in \{1,\dots,K\}$ denote the number of updates to the behavior policy μ and let $\rho_i(s,a) = \dfrac{\pi_i(a|s)}{\mu(a|s)}$ be the per-step IS weight. Using the variance state-action function $M_{\pi_i}^{\mu_k}(s,a)$, the behavior policy updates as follows:*

$$\mu_{k+1}(a|s) = \frac{\sqrt{\sum_i \pi_i(a|s)^2 M_{\pi_i}^{\mu_k}(s,a)}}{\sum_{a'} \sqrt{\sum_i \pi_i(a'|s)^2 M_{\pi_i}^{\mu_k}(s,a')}}. \tag{3}$$

Proof. The proof is presented in App. A.1. □

Theorem 4.1 describes how to iteratively update the behavior policy μ_k by using the return variance $M_{\pi_i}^{\mu_k}$. The policy μ_{k+1} selects actions proportional to their variance, meaning high-variance return (s,a) pairs are explored frequently. By visiting high-variance return pairs, policy gains informative samples and reduce the overall uncertainty. Consequently, this process improves the GVF value predictions and decrease the number of interactions needed for effective learning.

Next Theorem 4.2 shows that each behavior policy update either decreases or maintains the overall variance across GVFs, ensuring consistent progress towards minimizing variance without oscillation. In simple terms, each policy update ensures either stability or improvement in data collection and value estimation efficiency.

Theorem 4.2. ***(Behavior Policy Improvement:)*** *The behavior policy update in Eq.(3) ensures that the aggregated variances across all target policies $\pi_{i\in\{1\ldots\mathcal{N}\}}$ decrease with each update step $k \in \{1 \ldots K\}$, that is,*

$$\sum_{i=1}^{\mathcal{N}} M_{\pi_i}^{\mu_{k+1}} \leq \sum_{i=1}^{\mathcal{N}} M_{\pi_i}^{\mu_k}, \forall k.$$

Proof. The proof is in App. A.1. □

5 Variance Function

The theorems provided in the previous section rely on the variance function $M_{\pi_i}^{\mu_k}$. Here, we study this variance function in detail.

What is the Variance Function M? In an off-policy context [Sherstan et al. (2018), Jain et al. (2021)], introduced the variance function M, which estimates the variance in return under a target policy π using data from a different behavior policy μ. We will directly use this function M as our variance estimator and present it here for completeness. The function M for a state-action pair under π, with an importance sampling correction factor $\rho_t = \frac{\pi(a_t|s_t)}{\mu(a_t|s_t)}$, is defined as:

$$M_\pi^\mu(s,a) = \text{Var}_{a\sim\mu}\left(G_{t,\pi}|s_t = s, a_t = a\right) = \mathbb{E}_{a\sim\mu}\left[\delta_t^2 + \gamma^2\rho_{t+1}^2 M_\pi^\mu(s_{t+1}, a_{t+1})|s_t = s, a_t = a\right] \tag{4}$$

Here, $G_{t,\pi}$ is the return at time t, and $\delta_t = r_t + \gamma\mathbb{E}_{a'\sim\pi}[Q_\pi(s_{t+1}, a')] - Q_\pi(s_t, a_t)$ is the TD error. We use **Expected Sarsa** (Sutton & Barto, 2018) to compute δ_t, eliminating the need for IS by using the expected value of the next state-action pair under π for bootstrapping, thus stabilizing the update and lowering the variance. $M_\pi^\mu(s,a)$ relates the variance under π from the current state-action pair to the next, when sampled from μ. This allows effective bootstrapping and iterative update using TD style method. The state variance function is defined as $M_\pi^\mu(s) = \sum_a \mu(a|s)\rho^2(s,a)M_\pi^\mu(s,a)$.

Note, true Q_π is required to compute the TD error δ_t in Eq. (4). Following Sherstan et al. (2018), we substitute the value estimate $\hat{Q}$ for the true function Q_π to compute δ_t in Eq. (4). Additionally, we use variance estimates $\hat{M}_\pi^{\mu_k}$ to update the next step policy μ_{k+1} instead of true variance in Eq. (3). This approach is similar to *generalized policy iteration* (Sutton & Barto, 2018), which simultaneously updates value estimator and improves the policy.

Next, we prove the existence of M in Lemma 5.1, which was not covered in Jain et al. (2021). This proof establishes a loose upper bound on the IS ratio ρ, limiting the divergence of the behavior policy from the target policy for effective off-policy variance estimation. This aligns with methods like TRPO (Schulman et al., 2015) and Retrace (Munos et al., 2016), which stabilize policy updates by controlling divergence.

Lemma 5.1. ***(Variance Function M Existence:)*** *Given a discount factor $0 < \gamma \leq 1$, the variance function M exists, if the below condition satisfies, $\mathbb{E}_{a\sim\mu}\left[\rho^2(s,a)\right] < \frac{1}{\gamma^2}$ for all states.*

Proof. Proof in App. A.2. □

Note, the objective in Eq. (2), might violate the above constraint on ρ; we empirically clip ρ to mitigate this problem. Additionally, IS requires $\mu(a|s) = 0$ when $\pi(a|s) = 0$. We empirically ensure $\mu(a|s) > \varepsilon << 1$ for all actions. The same constraint is added for all the baselines for fair comparison.

6 Algorithm

We present `GVFExplorer` algorithm, detailed in Algorithm 1. Our approach uses two networks: Q_θ for value function and M_w for variance, each with $\mathcal{N}$ heads (one head for each GVF). Starting with

a randomly initialized behavior policy, the agent observes cumulants for $\mathcal{N}$ GVFs at each step and updates Q_θ using off-policy TD. We use **Expected Sarsa** (Sutton & Barto, 2018) for both Q and M, eliminating off-policy corrections. The target Q updates follow:

$$Q_{tar}(s_t, a_t, s_{t+1}) = c_t + \gamma \sum_{a'} \pi(a'|s_{t+1}) Q_\theta(s_{t+1}, a'). \tag{5}$$

We use the TD error from Q learning, $\delta_Q = Q_{tar} - Q_\theta$, to update target M,

$$M_{tar}(s_t, a_t, s_{t+1}) = \delta_Q^2 + \gamma^2 \sum_{a'} \pi(a'|s_{t+1}) M_w(s_{t+1}, a'). \tag{6}$$

Both networks are updated via MSE loss. The behavior policy is iteratively updated using the new variance estimates for K steps, with learned Q values used for MSE metrics in Eq. (1).

To ensure reliable estimates, we initialize M values to small non-zero constants and apply epsilon exploration, which decays over time, ensuring coverage of the state-action space. This guarantees that agents visit a broad range of state-action pairs early on, preventing issues of zero variance for unvisited pairs. We applied epsilon-exploration to both `GVFExplorer` and the baselines for fair comparison.

We also use techniques like Experience Replay Buffer for data reuse and target networks for both Q and M to improve learning stability. Expected Sarsa is used consistently across all baselines for fair comparison. Refer Algorithm 1 for further details.

Algorithm 1: `GVFExplorer`: Efficient Behavior Policy Iteration for Multiple GVFs Evaluations

Input: Target policies $\pi_{i\in\{1,\dots n\}}$, initialized behavior policy μ_1, replay buffer $\mathcal{D}$, primary networks Q_θ, M_w (small non-zero M), target networks $Q_{\bar\theta}, M_{\bar w}$, learning rates α_Q, α_M, mini-batch size b, trajectory length T, target update frequency $l = 100$, value/variance update frequencies $p = 4$, $m = 8$, training steps K, exploration rates $\varepsilon_0, \varepsilon_{\text{decay}}, \varepsilon_{\min}$

for *environment step* $k = 1, \dots K$ **do**
  Set exploration rate: $\varepsilon_k = \max(\varepsilon_{\min}, \varepsilon_0 \cdot \varepsilon_{\text{decay}}^k)$
  Select action $a_t \sim \varepsilon$-greedy policy $\mu_k(\cdot|s_t)$
  Observe next state s_{t+1} and cumulants $c_t = \textit{Vector(size}(n))$
  Store transition (s_t, a_t, s_{t+1}, c_t) in $\mathcal{D}$
  if $step\%p == 0$ **then**
    //Update the Value Q_θ network
    Sample mini-batch of size b of transition $(s_t, a_t, s_{t+1}, c_t) \sim \mathcal{D}$.
    Update Q_θ using MSE loss $(Q_{tar}(s_t, a_t) - Q_\theta(s_t, a_t))^2$, where Q_{tar} is Eq. (5).
  end
  if $step\%m == 0$ **then**
    //Update the Variance M_w network
    Sample mini-batch of size b of transition $(s_t, a_t, s_{t+1}, c_t) \sim \mathcal{D}$
    Update M_w using MSE loss $(M_{tar}(s_t, a_t) - M_w(s_t, a_t))^2$, where M_{tar} is Eq. (6).
  end
  if $step\%l == 0$ **then**
    $\bar w = w$ and $\bar\theta = \theta$ //Update both target networks weights
  end
  //Update the behavior policy μ using the new Variance M_w
  Behavior policy becomes: $\mu_{k+1}(a|s) = \dfrac{\sqrt{\sum_{i=1}^n \pi_i(a|s)^2 M_w^i(s,a)}}{\sum_{a'\in\mathcal{A}} \sqrt{\sum_{i=1}^n \pi_i(a'|s)^2 M_w^i(s,a')}}, \forall s \in \mathcal{S}, a \in \mathcal{A}.$
end
Returns GVFs Values $V_i(s) = \sum_a \pi_i(a|s) Q_\theta^i(s,a)$ for $i = \{1, \dots, n\}$

7 Experiments

We investigate the empirical utility of our proposed algorithm in both discrete and continuous state environments. Our experiments are designed to answer the following questions: (a) How does

GVFExplorer compare with the different baselines (explained below) in terms of convergence speed and estimation quality? (b) Can GVFExplorer handle a large number of GVFs evaluations? (c) Can GVFExplorer work with non-stationary GVFs which change with time? (d) Can GVFExplorer work with non-linear function approximations and complex Mujoco environments? [1]

Baselines. We use Off-policy Expected Sarsa updates for parallel GVF estimations for all the experiments (including baselines) for fair comparison. We benchmark against several different **baselines**: (1) RoundRobin: uses a round-robin strategy sampling episodically from all target policies (2) MixturePolicy: Aggregated policy sampling from all target policies; (3) SR: a Successor Representation (SR) method using intrinsic reward of total change in SR and reward weights to learn behavior policy (McLeod et al., 2021). (4) BPS: behavior policy search method originally designed for single policy evaluation using a REINFORCE variance estimator (Hanna et al., 2017); we adapted it by averaging variance across multiple GVFs (similar to our objective). BPS results are limited to tabular settings due to scalability issues with it. (5) UniformPolicy: a uniform sampling policy over the action space. Implementation details and hyperparameters are in App. B.

Type of Cumulants. We experiment with three different types of cumulants, similar to McLeod et al. (2021) – **constant** with a fixed value; **distractor**, a *stationary* signal with fixed mean and constant variance (normal distribution); **drifter**, a *non-stationary* cumulant with zero-mean random walk with low variance (vary with time). Further description of cumulants is in App. B.2.

Experimental Settings. To answer the questions presented above, we consider different settings: **(Two Distinct Policies & Identical Cumulants):** In a tabular setting, we examine two GVFs with distinct target policies but identical *distractor cumulant*, $(\pi_1, c), (\pi_2, c)$. **(Two Distinct Policies & Distinct Cumulants):** In the same environment, we assess two GVFs with distinct target policy and distinct *distractor cumulant* with different fixed means, $(\pi_1, c_1), (\pi_2, c_2)$. **(Large Scale Evaluation with** 40 **distinct GVFs):** To verify the scalability of proposed method with high number of GVFs, we evaluate combinations of 4 different target policies $\pi_1 \dots \pi_4$ with 10 different *constant cumulants* $c_1 \dots c_{10}$, resulting in 40 GVFs. **(Non-Stationary Cumulants in FourRooms):** In FourRooms environment, we assess with two distinct GVFs - stationary distractor and non-stationary *drifter cumulant* – $(\pi_1, c_1), (\pi_2, c_2)$. **(Non-Linear Function Approximation):** In a continuous state environment with non-linear function approximator, we evaluate two distinct *distractor* GVFs, $(\pi_1, c_1), (\pi_2, c_2)$. **(Mujoco environments):** In Mujoco environments – walker and cheetah – evaluate different GVF tasks like walk, run and flip. Across these varied settings, we measure the averaged MSE across multiple GVFs.

7.1 Tabular Experiments

We conducted experiments in 20×20 gridworld with four cardinal actions and a tabular 20×20 FourRooms environment for added complexity. The discount factor is $\gamma = 0.99$, and the environment is stochastic with a 0.1 probability of random movement. The cumulants are zero everywhere except for at the goals. Episode terminates after 500 steps or upon reaching the goal. True value function for MSE computation is calculated analytically $V_\pi = (I - \gamma P_\pi)^{-1} c_\pi$. Detailed description of target policies and cumulants is provided in App. B.3. Table 1 summarizes the below results for tabular experiments.

In **Two Distinct Policies & Identical Cumulants**, we consider gridworld environment with *distractor* cumulant at top left corner with a reward drawn from normal distribution. Fig. 1a shows the averaged MSE across the two GVFs, with GVFExplorer showing much lower MSE compared to baselines.

Next, in **Two Distinct Policies & Distinct Cumulants**, we consider two distinct *distractor* cumulant (with different mean) GVFs placed at top-left and top-right corner respectively. Fig. 2a shows GVFExplorer with reduced MSEs compared to baselines. Figs. 2b and 2c qualitatively analyze the average absolute difference between true and estimated GVF values across states, $\mathbb{E}_i[|V_{\pi_i}^{c_i} - \hat{V}_{\pi_i}^{c_i}|]$, showing smaller errors (duller colors) for GVFExplorer. Fig. 8 (in App. B.3.2) presents the individual variance and MSE for both GVFs in GVFExplorer. Further, we conduct an ablation study to experiment with how GVFExplorer performance changes with poorer feature approximations.

[1] The code is available at Github.

Fig. 10 (in App. B.3.3) shows that MSE increases as the feature quality deteriorates, but `GVFExplorer` remains robust with moderately coarse approximations.

For **Non-Stationary Cumulant in FourRooms**, we evaluate the performance in FourRooms (FR) environment (Sutton et al., 1999) with two distinct GVFs: stationary **distractor** cumulant and a non-stationary **drifter** cumulant which changes value over time. As shown in Fig. 1b, `GVFExplorer` reduces MSE faster than other baselines, even with the non-stationary cumulant. Fig. 11 (in App. B.3.4) demonstrates the effectiveness of `GVFExplorer` in tracking the non-stationary cumulant signal in the later stages of learning.

In **Large Scale Evaluation with 40 Distinct GVFs**, we evaluate our method's scalability to large number of GVFs (refer App. B.3.5). We use **constant** cumulants with values ranging in $[50, 100]$. Fig. 1c compares the average MSE across the GVFs, showing that `GVFExplorer` scales well with an increasing number of GVFs. In contrast, the `SR` baseline struggles with scalability due to the varying cumulant scales affecting the intrinsic reward (the summation of all SRs and reward weights) of behavior policy.

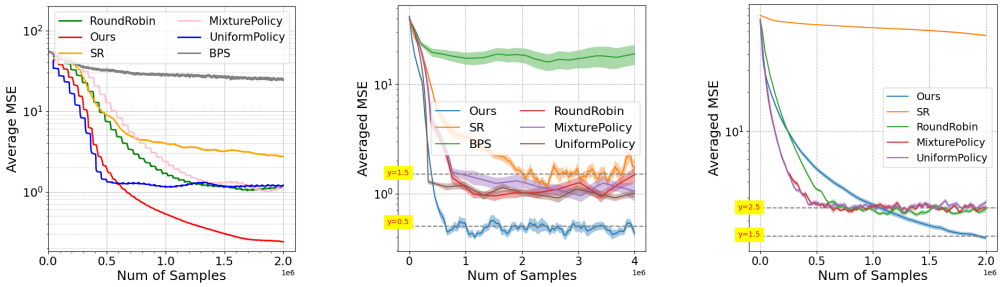

(a) **Two Distinct Policies & Identical Cumulants** (b) **Non-Stationary Cumulant in FourRooms** (c) **Large Scale Evaluation with 40 Distinct GVFs**

Figure 1: **MSE Performance**: Averaged MSE over 25 runs with standard error in different experimental settings. `GVFExplorer` demonstrate notably lower MSE compared to the baselines.

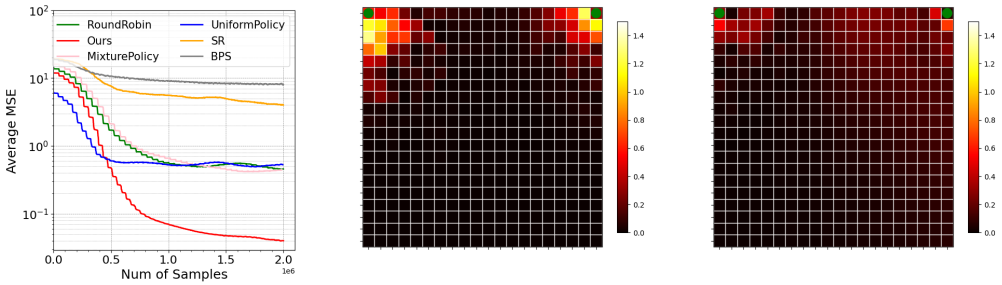

(a) Averaged MSE (b) Value Error (`RoundRobin`) (c) Value Error (`GVFExplorer`)

Figure 2: **Two Distinct Policies & Distinct Cumulants**: Evaluate averaged MSE over 25 runs with two distinct distractor GVFs $(\pi_1, c_1), (\pi_2, c_2)$ in gridworld . Green dots at top show two GVF goals. (a) Averaged MSE, (b) averaged absolute error in GVFs value predictions for baseline `RoundRobin` and (c) `GVFExplorer`. *The color bar uses log scale & vibrant colors indicate higher values.*

7.2 Continuous State Environment with Non-Linear Function Approximation

We use a continuous grid environment that extends the tabular experiments to a continuous state space (similar to McLeod et al. (2021)) and four discrete actions. For **Non-Linear Function Approximation**, we consider two distinct GVFs with distractor cumulants. An **Experience Replay Buffer** with a capacity of 25K and a batch size of 64 is used for all experiments. Further details on computing true value functions using Monte Carlo and network architectures are in App. B.4.

Prioritized Experience Replay (PER). We integrate PER (Schaul et al., 2015) to evaluate the effectiveness of our algorithm. Unlike the standard Experience Replay Buffer, which uniformly samples experiences, PER assigns priorities based on the TD error magnitude in the Q-network. PER and `GVFExplorer` are complementary approaches: PER re-weights the collected data in replay buffer based on the priority, while `GVFExplorer` adjusts the behavior policy to influence data collection.

Combining PER with `GVFExplorer` drastically lowers MSE compared to other baselines (even when compared to all baselines + PER). We use the absolute sum of TD errors across multiple GVF Q-functions as a priority metric for PER in all baselines, including `GVFExplorer`. Placing the priority on the TD error of the variance function in `GVFExplorer` yields less favorable results compared to priority on Q-function's TD error. In Fig. 3, we present the MSE for both standard experience replay (solid lines) and PER (dotted lines) for all algorithms. PER generally reduces MSE, but its integration with `GVFExplorer` shows much lower MSE. This is likely as `GVFExplorer` could over-sample high variance return samples, causing a skewed buffer distribution. PER's non-uniform sampling maintains a balanced data distribution, which helps in stringent MSE reduction. For the `SR` baseline, using the TD error in SR predictions as a priority for PER led to performance degradation, suggesting non-stationarity in SRs' TD errors might mislead PER to prioritize less relevant states under the current policy. The original `SR` work by McLeod et al. (2021) does not use PER in the experiments. For PER scenario, we qualitatively compare the absolute value error for baseline `RoundRobin` and `GVFExplorer` by discretizing the state space in Figs. 3b and 3c and observe that our algorithms results in smaller value prediction error. Further insights into the variance estimation by `GVFExplorer` is shown in Figs. 15 and 16 (App. B.4). Table 3((App. B.4) summarizes the results highlighting the performance of various algorithms.

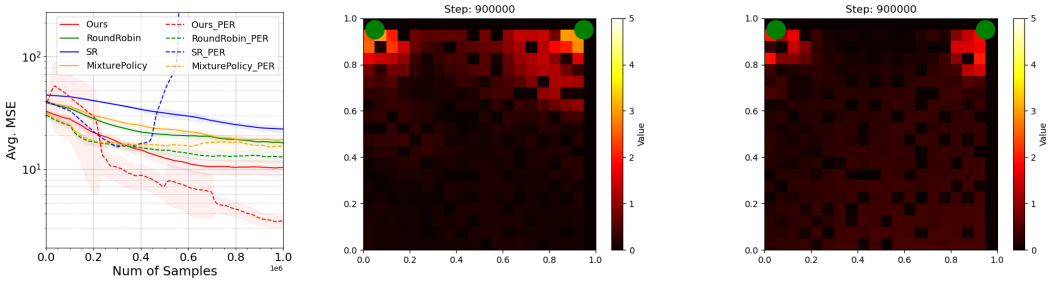

(a) Avg. MSE (b) Value error (`RoundRobin`) (c) Value error (`GVFExplorer`)

Figure 3: **Non-Linear Function Approximation**: (a) Averaged MSE over 50 runs with standard error using **Experience Replay Buffer** (solid lines) and **PER** (dotted lines). `GVFExplorer` show lower MSE with both buffers. PER generally reduces MSE across all algorithms except `SR`. Log-scale absolute value error for `RoundRobin` (b) and `GVFExplorer` (c); `GVFExplorer` achieves smaller errors (vibrant colors represent higher values).

7.3 Mujoco Environments with Continuous State-Actions Tasks

We use DM-Control (Tassa et al., 2018) based continuous state-action tasks to experiment with Mujoco environments, *Walker* and *Cheetah* domain. To expand the proposed method to continuous action environments, any policy-gradient (PG) based algorithm can be used. In our experiments, we use Soft Actor-Critic (SAC) algorithm (Haarnoja et al., 2018) as a base PG method to incorporate the proposed variance-minimization objective.

A separate network for variance estimation is added to SAC. Further implementation details are provided in App. B.5. To experiment in *Walker* environment, we use two GVF tasks, namely walk and flip. Similarly, for *Cheetah* environment, we use walk and run GVF tasks. We also added KL regularize between the learned behavior policy and the given GVFs target policies to prevent divergence. We use MC to compute the true Q-value GVF estimates and compare the MSE between these MC values and the Q-critic network. We use the same Q-critic architecture for the baseline algorithms – `UniformPolicy` and `RoundRobin` – for fair comparison. In Fig. 4 we observe that `GVFExplorer` reduces MSE faster than the baselines.

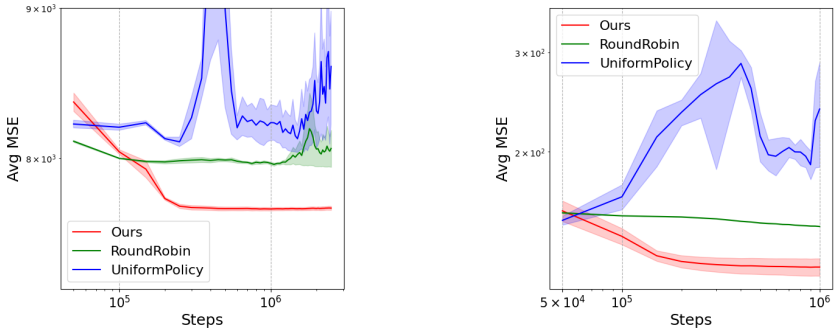

(a) Averaged MSE in Walker

(b) Averaged MSE in Cheetah

Figure 4: **MSE in Mujoco**: Averaged MSE over 5 runs with standard error in Mujoco environment with continuous state-actions for (a)Walker and (b)Cheetah domains for `GVFExplorer`, `UniformPolicy` and `RoundRobin`. `GVFExplorer` consistently lowers averaged MSE as compared to the baselines.

8 Discussion

We addressed the problem of parallel evaluations of multiple GVFs, each conditioned on a given target policy and cumulant. We developed a method to adaptively learn a behavior policy that uses a single experience stream to estimate all GVF values in parallel. The resulting behavior policy update selects the actions in proportion to the total variance of the return across GVFs. This guides the policy to frequently explore less understood areas (high variance in return), which helps to better estimate the mean return with fewer samples. Therefore, our approach lowers the overall MSE in GVF predictions and uses fewer interactions. We theoretically proved that each behavior policy update reduces the total prediction error. Empirically, we showed that `GVFExplorer` scales effectively with an increasing number of distinct GVFs, robustly handles non-stationary cumulants in a tabular setting, and adapts well to non-linear function approximation. Further, we also demonstrated the performance in complex continuous state-action Mujoco environments by showing that `GVFExplorer` can be combined effectively with any existing policy-gradient methods.

Limitations and Future Work. One notable drawback of `GVFExplorer` is the increased time complexity, due to simultaneously learning two networks for value and variance estimation respectively. Additionally, `GVFExplorer` has not been evaluated in environments with significant difference in the cumulant value range. Such disparities could lead to varying variances, potentially resulting in oversampling areas with higher cumulant values. Calibration across cumulants may be necessary in these cases.

In this work we focused on minimizing the total MSE, but other loss functions, such as weighted MSE could also be considered. However, weighted MSE requires a priori knowledge about the weighting of errors in different GVFs, which is not readily available. A potential future direction could be to use variance scales to automatically adjust these weights, in order to provide uniform MSE reduction across all GVFs. Looking ahead, we are interested in testing our approach with multi-dimensional cumulants and general state-dependent discount factors, as well as, extending the applicability of `GVFExplorer` to control settings where the target policies are unknown.

References

András Antos, Varun Grover, and Csaba Szepesvári. Active learning in multi-armed bandits. In *Algorithmic Learning Theory: 19th International Conference, ALT 2008, Budapest, Hungary, October 13-16, 2008. Proceedings 19*, pp. 287–302. Springer, 2008.

Pierre-Luc Bacon. *Temporal Representation Learning*. McGill University (Canada), 2018.

Yuri Burda, Harrison Edwards, Amos Storkey, and Oleg Klimov. Exploration by random network distillation, 2018.

Alexandra Carpentier, Remi Munos, and András Antos. Adaptive strategy for stratified monte carlo sampling. *J. Mach. Learn. Res.*, 16:2231–2271, 2015.

Peter Dayan. Improving generalization for temporal difference learning: The successor representation. *Neural computation*, 5(4):613–624, 1993.

Thomas Degris, Martha White, and Richard S Sutton. Off-policy actor-critic. *arXiv preprint arXiv:1205.4839*, 2012.

Benjamin Eysenbach, Abhishek Gupta, Julian Ibarz, and Sergey Levine. Diversity is all you need: Learning skills without a reward function. *arXiv preprint arXiv:1802.06070*, 2018.

Jordan Frank, Shie Mannor, and Doina Precup. Reinforcement learning in the presence of rare events. In *Proceedings of the 25th international conference on Machine learning*, pp. 336–343, 2008.

Zhaohan Guo, Shantanu Thakoor, Miruna Pîslar, Bernardo Avila Pires, Florent Altché, Corentin Tallec, Alaa Saade, Daniele Calandriello, Jean-Bastien Grill, Yunhao Tang, et al. Byol-explore: Exploration by bootstrapped prediction. *Advances in neural information processing systems*, 35: 31855–31870, 2022.

Tuomas Haarnoja, Aurick Zhou, Pieter Abbeel, and Sergey Levine. Soft actor-critic: Off-policy maximum entropy deep reinforcement learning with a stochastic actor. In *International conference on machine learning*, pp. 1861–1870. PMLR, 2018.

Josiah P Hanna, Philip S Thomas, Peter Stone, and Scott Niekum. Data-efficient policy evaluation through behavior policy search. In *International Conference on Machine Learning*, pp. 1394–1403. PMLR, 2017.

Timothy Classen Hesterberg. *Advances in importance sampling*. Stanford University, 1988.

Max Jaderberg, Volodymyr Mnih, Wojciech Marian Czarnecki, Tom Schaul, Joel Z Leibo, David Silver, and Koray Kavukcuoglu. Reinforcement learning with unsupervised auxiliary tasks. *arXiv preprint arXiv:1611.05397*, 2016.

Arushi Jain, Gandharv Patil, Ayush Jain, Khimya Khetarpal, and Doina Precup. Variance penalized on-policy and off-policy actor-critic. In *Proceedings of the AAAI Conference on Artificial Intelligence*, volume 35, pp. 7899–7907, 2021.

Herman Kahn and Andy W Marshall. Methods of reducing sample size in monte carlo computations. *Journal of the Operations Research Society of America*, 1(5):263–278, 1953.

Pawel Ladosz, Lilian Weng, Minwoo Kim, and Hyondong Oh. Exploration in deep reinforcement learning: A survey. *Information Fusion*, 85:1–22, 2022.

Xinyu Li, Zachary C Lipton, and Liu Leqi. Personalized language modeling from personalized human feedback. *arXiv preprint arXiv:2402.05133*, 2024.

Cam Linke, Nadia M Ady, Martha White, Thomas Degris, and Adam White. Adapting behavior via intrinsic reward: A survey and empirical study. *Journal of artificial intelligence research*, 69: 1287–1332, 2020.

Marlos C Machado, Clemens Rosenbaum, Xiaoxiao Guo, Miao Liu, Gerald Tesauro, and Murray Campbell. Eigenoption discovery through the deep successor representation. *arXiv preprint arXiv:1710.11089*, 2017.

Matthew McLeod, Chunlok Lo, Matthew Schlegel, Andrew Jacobsen, Raksha Kumaraswamy, Martha White, and Adam White. Continual auxiliary task learning. *Advances in Neural Information Processing Systems*, 34:12549–12562, 2021.

Alberto Maria Metelli, Samuele Meta, and Marcello Restelli. On the relation between policy improvement and off-policy minimum-variance policy evaluation. In *Uncertainty in Artificial Intelligence*, pp. 1423–1433. PMLR, 2023.

Rémi Munos, Tom Stepleton, Anna Harutyunyan, and Marc Bellemare. Safe and efficient off-policy reinforcement learning. *Advances in neural information processing systems*, 29, 2016.

Pierre-Yves Oudeyer, Frdric Kaplan, and Verena V Hafner. Intrinsic motivation systems for autonomous mental development. *IEEE transactions on evolutionary computation*, 11(2):265–286, 2007.

Art B Owen. Monte carlo theory, methods and examples, 2013.

Javier Parapar and Filip Radlinski. Diverse user preference elicitation with multi-armed bandits. In *Proceedings of the 14th ACM international conference on web search and data mining*, pp. 130–138, 2021.

Doina Precup. Eligibility traces for off-policy policy evaluation. *Computer Science Department Faculty Publication Series*, pp. 80, 2000.

Martin L Puterman. *Markov decision processes: discrete stochastic dynamic programming*. John Wiley & Sons, 2014.

Reuven Y Rubinstein and Dirk P Kroese. *Simulation and the Monte Carlo method*. John Wiley & Sons, 2016.

Tom Schaul, John Quan, Ioannis Antonoglou, and David Silver. Prioritized experience replay. *arXiv preprint arXiv:1511.05952*, 2015.

Matthew Schlegel, Andrew Jacobsen, Zaheer Abbas, Andrew Patterson, Adam White, and Martha White. General value function networks. *Journal of Artificial Intelligence Research*, 70:497–543, 2021.

Jürgen Schmidhuber. Formal theory of creativity, fun, and intrinsic motivation (1990–2010). *IEEE transactions on autonomous mental development*, 2(3):230–247, 2010.

John Schulman, Sergey Levine, Pieter Abbeel, Michael Jordan, and Philipp Moritz. Trust region policy optimization. In *International conference on machine learning*, pp. 1889–1897. PMLR, 2015.

Craig Sherstan. Representation and general value functions. 2020.

Craig Sherstan, Dylan R Ashley, Brendan Bennett, Kenny Young, Adam White, Martha White, and Richard S Sutton. Comparing direct and indirect temporal-difference methods for estimating the variance of the return. In *UAI*, pp. 63–72, 2018.

Richard S Sutton and Andrew G Barto. *Reinforcement learning: An introduction*. MIT press, 2018.

Richard S Sutton, Doina Precup, and Satinder Singh. Between mdps and semi-mdps: A framework for temporal abstraction in reinforcement learning. *Artificial intelligence*, 112(1-2):181–211, 1999.

Richard S Sutton, Joseph Modayil, Michael Delp, Thomas Degris, Patrick M Pilarski, Adam White, and Doina Precup. Horde: A scalable real-time architecture for learning knowledge from unsupervised sensorimotor interaction. In *The 10th International Conference on Autonomous Agents and Multiagent Systems-Volume 2*, 2011.

Liang Tang, Yexi Jiang, Lei Li, Chunqiu Zeng, and Tao Li. Personalized recommendation via parameter-free contextual bandits. In *Proceedings of the 38th international ACM SIGIR conference on research and development in information retrieval*, pp. 323–332, 2015.

Yuval Tassa, Yotam Doron, Alistair Muldal, Tom Erez, Yazhe Li, Diego de Las Casas, David Budden, Abbas Abdolmaleki, Josh Merel, Andrew Lefrancq, et al. Deepmind control suite. *arXiv preprint arXiv:1801.00690*, 2018.

David S Watkins. *Fundamentals of matrix computations*. John Wiley & Sons, 2004.

Adam White et al. Developing a predictive approach to knowledge. 2015.

Ronald J Williams. Simple statistical gradient-following algorithms for connectionist reinforcement learning. *Machine learning*, 8:229–256, 1992.

Tengyu Xu, Zhuoran Yang, Zhaoran Wang, and Yingbin Liang. A unifying framework of off-policy general value function evaluation. *Advances in Neural Information Processing Systems*, 35: 13570–13583, 2022.

A Proofs

A.1 Behavior Policy Update Theorems

Theorem 4.1. ***(Behavior Policy Update:)*** *Given $\mathcal{N}$ target policies π_i for $i \in \{1 \dots \mathcal{N}\}$, let $k \in \{1, \dots, K\}$ denote the number of updates to the behavior policy μ and let $\rho_i(s,a) = \dfrac{\pi_i(a|s)}{\mu(a|s)}$ be the per-step IS weight. Using the variance state-action function $M^{\mu_k}_{\pi_i}(s,a)$, the behavior policy updates as follows:*

$$\mu_{k+1}(a|s) = \frac{\sqrt{\sum_i \pi_i(a|s)^2 M^{\mu_k}_{\pi_i}(s,a)}}{\sum_{a'} \sqrt{\sum_i \pi_i(a'|s)^2 M^{\mu_k}_{\pi_i}(s,a')}}. \tag{3}$$

Proof. We formulate Eq. (2) as a Lagrangian equation below to solve for the optimal behavior policy μ^*.

$$\mathcal{L}(\mu, \lambda_{s,a}, w_s) = \underbrace{\sum_i \sum_s d(s) M^{\mu}_{\pi_i}(s)}_{\text{I part}} + \underbrace{\sum_{s,a} \lambda_{s,a} \mu(s,a)}_{\text{II part}} + \underbrace{\sum_s w_s (1 - \sum_a \mu(s,a))}_{\text{III part}}. \tag{7}$$

Here, $\lambda \in \mathbb{R}^{|\mathcal{S} \times \mathcal{A}|}$ and $\mathbf{w} \in \mathbb{R}^{|\mathcal{S}|}$ denotes the Lagrangian multipliers. The following KKT conditions satisfy:

1. $\nabla_{\mu(s,a)} \mathcal{L} = 0$
2. $\lambda_{s,a} \mu(s,a) = 0$
3. $\lambda_{s,a} \geq 0$
4. $\mu(s,a) \geq 0$
5. $\sum_a \mu(s,a) = 1$

Gradient of ρ. The gradient of $\rho(s,a)$ w.r.t. $\mu(a|s)$,

$$\nabla_{\mu(s,a)} \rho(s,a) = \frac{\pi(a|s)}{\nabla \mu(a|s)} = -\frac{\pi(a|s)}{\mu(a|s)^2} = -\frac{\rho(s,a)}{\mu(a|s)}.$$

Solving I part. We will compute the gradient of $M^{\mu}_{\pi_i}(s)$ in Eq. (4) w.r.t to given $\mu(s,a)$. Here, $\rho(s,a) = \frac{\pi(a|s)}{\mu(a|s)}$ is IS weight. We expand $M^{\mu}_{\pi_i}(s)$ relation with $M^{\mu}_{\pi_i}(s,a)$ to derive the gradient,

$$\begin{aligned}
M^{\mu}_{\pi_i}(\tilde{s}) &= \sum_{\tilde{a}} \mu(\tilde{a}|\tilde{s}) \rho_i(\tilde{s},\tilde{a})^2 M^{\mu}_{\pi_i}(\tilde{s},\tilde{a}) \\
\nabla_{\mu(s,a)} M^{\mu}_{\pi_i}(\tilde{s}) &= \nabla_{\mu(s,a)} \left\{ \sum_{\tilde{a}} \mu(\tilde{a}|\tilde{s}) \rho_i(\tilde{s},\tilde{a})^2 M^{\mu}_{\pi_i}(\tilde{s},\tilde{a}) \right\} \\
&= \rho_i(s,a)^2 M^{\mu}_{\pi_i}(s,a) + 2\mu(a|s)\rho_i(s,a) \underbrace{\nabla \rho_i(s,a)}_{=-\frac{\rho_i(s,a)}{\mu(a|s)}} M^{\mu}_{\pi_i}(s,a) + \underbrace{\mu(a|s)\rho_i(s,a)^2 \nabla_{\mu} M^{\mu}_{\pi_i}(s,a)}_{=\text{IV part}} \\
&= \rho_i(s,a)^2 M^{\mu}_{\pi_i}(s,a) - 2\rho_i(s,a)^2 M^{\mu}_{\pi_i}(s,a) \\
&= -\rho_i(s,a)^2 M^{\mu}_{\pi_i}(s,a).
\end{aligned}$$

The final term $\nabla_{\mu} M^{\mu}_{\pi_i}(s,a)$ is difficult to estimate in an iterative off-policy setting. Hence, we are omitting (*IV part*) from the above gradient, which is similar to Degris et al. (2012)[Sec 2.2], where the gradient of $Q(s,a)$ was omitted while deriving the policy update.

Solving for the Lagrangian Eq. (7) further by substituting the (*I part*), and taking derivation of II & III part and using the (1) KKT condition.

$$\nabla_{\mu(s,a)} \mathcal{L}(\mu, \lambda_{s,a}, w_s) = -\sum_i d(s) \rho_i(s,a)^2 M^{\mu}_{\pi_i}(s,a) + \lambda_{s,a} - w_s = 0. \tag{8}$$

From (2)KKT condition, we know that either $\lambda_{s,a} = 0$ or $\mu(a|s) = 0$. Following the arguments of IS, support for $\mu(a|s)$ can only be 0 when the support for target policy $\pi(a|s) = 0$. Solving for the case when support for target policy in non-zero, then let $\lambda_{s,a} = 0$. We can simplify the gradient of Lagrangian in Eq. (8),

$$\begin{aligned} w_s &= -\sum_i d(s)\rho_i(s,a)^2 M^{\mu}_{\pi_i}(s,a) = -\sum_i d(s)\frac{\pi_i(a|s)^2}{\mu(a|s)^2} M^{\mu}_{\pi_i}(s,a) \\ \mu(a|s) &= \sqrt{\frac{\sum_i \pi_i(a|s)^2 M^{\mu}_{\pi_i}(s,a)}{-w_s/d(s)}} \end{aligned} \tag{9}$$

We know that the numerator is always positive (variance M is positive), therefore $w_s < 0$. Let $y_s = -w_s/d(s)$. From condition (5), we know that $\sum_a \mu(a|s) = 1$. Using Eq. (9) and summing over all the actions we get,

$$\sum_a \mu(a|s) = \sum_a \sqrt{\frac{\sum_i \pi_i(a|s)^2 M^{\mu}_{\pi_i}(s,a)}{y_s}} = 1$$

$$\text{Hence, } \sqrt{y_s} = \sum_a \sqrt{\sum_i \pi_i(a|s)^2 M^{\mu}_{\pi_i}(s,a)}.$$

Therefore, the update for optimal behavior policy becomes,

$$\mu(a|s)^* = \frac{\sqrt{\sum_i \pi_i(a|s)^2 M^{\mu^*}_{\pi_i}(s,a)}}{\sum_a \sqrt{\sum_i \pi_i(a|s)^2 M^{\mu^*}_{\pi_i}(s,a)}}.$$

As the optimal policy μ^* appear on both the sides, this can be interpreted as an iterative update, where k denotes the iterate number.

$$\mu_{k+1}(a|s) = \frac{\sqrt{\sum_i \pi_i(a|s)^2 M^{\mu_k}_{\pi_i}(s,a)}}{\sum_a \sqrt{\sum_i \pi_i(a|s)^2 M^{\mu_k}_{\pi_i}(s,a)}}.$$

□

Theorem 4.2. ***(Behavior Policy Improvement:)*** *The behavior policy update in Eq.(3) ensures that the aggregated variances across all target policies $\pi_{i\in\{1\ldots\mathcal{N}\}}$ decrease with each update step $k \in \{1\ldots K\}$, that is,*

$$\sum_{i=1}^{\mathcal{N}} M^{\mu_{k+1}}_{\pi_i} \leq \sum_{i=1}^{\mathcal{N}} M^{\mu_k}_{\pi_i},\ \forall k.$$

Proof. Theorem 4.1 suggests, for any given μ_k behavior policy, the next successive approximation μ_{k+1} minimizes the objective function Eq. (2), i.e.,

$$\begin{aligned} \mu_{k+1} &= \min_{\mu} \sum_i \sum_s d(s) \underbrace{M^{\mu_k}_{\pi_i}(s)}_{=\mathrm{I}} \\ &= \min_{\mu} \sum_i \sum_s d(s) \underbrace{\sum_a \mu(a|s)\frac{\pi_i(a|s)^2}{\mu(a|s)^2} M^{\mu_k}_{\pi_i}(s,a)}_{=M^{\mu_k}_{\pi_i}(s)}. \end{aligned} \tag{10}$$

We will omit writing $d(s)$ and assume that $s \sim d(s)$. Further, we will use the notation $\rho^i_k(s,a) = \dfrac{\pi_i(a|s)}{\mu_k(a|s)}$ for ease of writing. From Eq. (10), we can establish the relation,

$$\underbrace{\sum_{i,s,a} \mu_k(a|s)\frac{\pi_i(a|s)^2}{\mu_k(a|s)^2} M^{\mu_k}_{\pi_i}(s,a)}_{=M^{\mu_k}_{\pi_i}(s)} \geq \sum_{i,s,a} \mu_{k+1}(a|s)\frac{\pi_i(a|s)^2}{\mu_{k+1}(a|s)^2} M^{\mu_k}_{\pi_i}(s,a). \tag{11}$$

Now, we will use Eq. (11) relation to further simplify the equation and establish that variance decreases with every update step k. We will use the notation $\rho_{t:t+n} = \Pi_{l=0}^{n} \rho_{t+l}$ to denote the products.

$$
\begin{aligned}
\sum_{i,s} M_{\pi_i}^{\mu_k}(s) &\geq \sum_{i,s,a} \mu_{k+1}(a|s) \rho_{k+1}^{i}(s,a)^2 M_{\pi_i}^{\mu_k}(s,a) \\
&= \sum_{i,s,a} \mu_{k+1}(a|s) \rho_{k+1}^{i}(s,a)^2 \mathbb{E}_{a\sim\mu_k}[\delta_t^2 + \gamma^2 M_{\pi_i}^{\mu_k}(s_{t+1}) | s_t = s] \\
&= \sum_{i,s} \mathbb{E}_{a\sim\mu_{k+1}} \left[(\rho_t^i)^2 \delta_t^2 + \gamma^2 (\rho_t^i)^2 \underbrace{M_{\pi_i}^{\mu_k}(s_{t+1})}_{\text{expand this}} | s_t = s \right] \\
&\geq \sum_{i,s} \mathbb{E}_{a\sim\mu_{k+1}} \left[(\rho_t^i)^2 \delta_t^2 + \gamma^2 (\rho_t^i)^2 \mathbb{E}_{a\sim\mu_{k+1}} \left[(\rho_{t+1}^i)^2 \delta_{t+1}^2 + \gamma^2 (\rho_{t+1}^i)^2 M_{\pi_i}^{\mu_k}(s_{t+2}) | s_{t+1} \right] | s_t = s \right] \\
&= \sum_{i,s} \mathbb{E}_{a\sim\mu_{k+1}} \left[(\rho_t^i)^2 \delta_t^2 + \gamma^2 (\rho_t^i)^2 (\rho_{t+1}^i)^2 \delta_{t+1}^2 + \gamma^4 (\rho_t^i)^2 (\rho_{t+1}^i)^2 M_{\pi_i}^{\mu_k}(s_{t+2}) | s_t = s \right] \\
&\vdots \\
&\geq \sum_{i,s} \mathbb{E}_{a\sim\mu_{k+1}} \left[\rho_{t:t}^2 \delta_t^2 + \gamma^2 (\rho_{t:t+1}^i)^2 \delta_{t+1}^2 + \gamma^4 (\rho_{t:t+2}^i)^2 \delta_{t+2}^2 + \ldots | s_t = s \right] \\
&\geq \sum_{i,s} M_{\pi_i}^{\mu_{k+1}}(s).
\end{aligned}
\tag{12}
$$

□

A.2 When does Variance Function Exists?

Let $\mathbf{c}_\mu \in \mathbb{R}^{|\mathcal{S}\times\mathcal{A}|}$ denote the pseudo-reward $\mathbf{c}_\mu(s,a) = \sum_{s'} P(s'|s,a)\delta^2(s,a,s')$ and $\bar{\mathbf{P}}_\mu \in \mathbb{R}^{|\mathcal{S}\times\mathcal{A}\times\mathcal{S}\times\mathcal{A}|}$ represent the transition probability matrix $\bar{\mathbf{P}}_\mu(s,a,s',a') = P(s'|s,a)\mu(a'|s')\rho^2(s',a')$. The matrix form of M_π^μ is:

$$
M_\pi^\mu = \mathbf{c}_\mu + \gamma^2 \bar{\mathbf{P}}_\mu M_\pi^\mu \implies M_\pi^\mu = (I - \gamma^2 \bar{\mathbf{P}}_\mu)^{-1} \mathbf{c}_\mu. \tag{13}
$$

The existence of M_π^μ hinges on the invertibility of matrix $(I - \gamma^2 \bar{\mathbf{P}}_\mu)$. Lemma 5.1 establishes the existence of the above inverse using Definition A.1 and Lemmas A.2 and A.3.

Definition A.1. (Spectral Radius) The spectral radius of a matrix $\mathbf{A} \in \mathbb{R}^{n\times n}$ is denoted by $sr(\mathbf{A}) = \max(\lambda_1, \lambda_2, \ldots, \lambda_n)$, where λ_i denotes the ith eigenvalue of $\mathbf{A}$.

Lemma A.2. *The spectral radius $sr(\mathbf{A})$ of a matrix $\mathbf{A} \in \mathbb{R}^{n\times n}$ follows the relation, $sr(\mathbf{A}) \leq \|\mathbf{A}\|$, where, $\|\mathbf{A}\| = \max_i \sum_j \mathbf{A}(i,j)$ is the infinity norm over a matrix.*

Proof. Following the derivation from Bacon (2018) Ph.D. thesis and work of Watkins (2004), we use the eigenvalue of a matrix to show that $sr(\mathbf{A}) < \|\mathbf{A}\|$. We can write $\lambda\mathbf{x} = \mathbf{A}\mathbf{x}$, when λ is the eigenvalue of $\mathbf{A}$. For any sub-multiplicative matrix norm, $\|\mathbf{AB}\| \leq \|\mathbf{A}\|\|\mathbf{B}\|$. Using this property,

$$
\begin{aligned}
\|\lambda\mathbf{x}\| = |\lambda|\|\mathbf{x}\| = \|\mathbf{A}\mathbf{x}\| &\leq \|\mathbf{A}\|\|\mathbf{x}\|, \\
|\lambda| &\leq \|\mathbf{A}\|.
\end{aligned}
$$

The above is true for any eigenvalue λ of $\mathbf{A}$. So this must also be true for the maximum eigenvalue of $\mathbf{A}$. Therefore, we can express,

$$
sr(\mathbf{A}) \leq \|A\|.
$$

□

Lemma A.3. *When the spectral radius of $sr(\mathbf{A}) < 1$, then $(I - \mathbf{A})^{-1}$ exits and is equal to, $(I - \mathbf{A})^{-1} = \sum_{t=0}^{\infty} \mathbf{A}^t$.*

Proof. The proof for the Lemma is presented in Puterman (2014)[Proposition A.3]. □

Lemma 5.1. ***(Variance Function M Existence:)*** *Given a discount factor $0 < \gamma \leq 1$, the variance function M exists, if the below condition satisfies, $\mathbb{E}_{a\sim\mu}\left[\rho^2(s,a)\right] < \frac{1}{\gamma^2}$ for all states.*

Proof. Following Lemma A.3, the existence of M hinges on the existence of inverse $(I - \gamma^2\bar{\mathbf{P}}_\mu)^{-1}$. Further, $(I - \gamma^2\bar{\mathbf{P}}_\mu)^{-1}$ exists if spectral radius $sr(\gamma^2\bar{\mathbf{P}}_\mu) < 1$. Further, from Lemma A.2, we know that for any given matrix $\mathbf{A}$, spectral radius satisfies, $sr(\mathbf{A}) \leq \|A\|$. Hence, using the above two lemmas, we can express,

$$sr(\gamma^2\bar{\mathbf{P}}_\mu) \leq \|\gamma^2\bar{\mathbf{P}}_\mu\| \leq \gamma^2\|\bar{\mathbf{P}}_\mu\|.$$

Further, if spectral radius satisfies the below condition, then the inverse exists,

$$sr(\gamma^2\bar{\mathbf{P}}_\mu) \leq \gamma^2\|\bar{\mathbf{P}}_\mu\| < 1.$$

We expand the middle infinity norm term and get

$$\max_{s,a}\sum_{s',a'}\bar{\mathbf{P}}_\mu(s,a,s',a') < \frac{1}{\gamma^2}$$
$$\max_{s,a}\sum_{s'}P(s'|s,a)\sum_{a'}\mu(a'|s')\rho^2(s',a') < \frac{1}{\gamma^2}.$$

We can further express the above condition as $\mathbb{E}_{a\sim\mu}\left[\rho(s,a)^2\right] < \frac{1}{\gamma^2}, \forall s \in \mathcal{S}$. □

B Experiments

This section provides detail about the experiments in the main paper as well as additional experiments in the Appendix. All the experiments require less than $1GB$ of memory and have used combined compute less than total 4 CPU months and 1 GPU month.

For all the experiments, we consider the two target policies with four cardinal directions left (L), right (R), up (U) and down (D) for the tabular and non-linear function approximation environments. These policies are specified as follows for every state $s \in \mathcal{S}$:

$$\begin{aligned}\pi_1(s) &= \{L: 0.175, R: 0.175, U: 0.25, D: 0.4\}\\ \pi_2(s) &= \{L: 0.25, R: 0.15, U: 0.25, D: 0.35\}.\end{aligned} \tag{14}$$

B.1 Baselines

(1) `RoundRobin`: We used a round robin strategy to sample data from all given n target policies episodically. We used Expected Sarsa to estimate all GVF value functions in parallel when a transition is given as $(s_t, a_t, s_{t+1}, c_{i=\{1,\ldots n\}})$,

$$Q_i(s_t,a_t) = Q_i(s_t,a_t) + \alpha\left(c_i(s_t,a_t) + \gamma\sum_a \pi_i(a'|s_{t+1})Q_i(s_{t+1},a') - Q_i(s_t,a_t))\right)$$

(2) `MixturePolicy`, `UniformPolicy` are also evaluated using Expected Sarsa. `MixturePolicy` is defined as,

$$\mu_{\text{Mixture}}(a|s) = \frac{\sum_{i=1}^{\mathcal{N}}\pi_i(a|s)}{\sum_{a'}\sum_{i=1}^{\mathcal{N}}\pi_i(a'|s)}.$$

(3) `SR`**:** Based on (McLeod et al., 2021), `SR` uses the summation of weight changes in the Successor Representation (SR) and reward weights to obtain the intrinsic reward for behavior policy updates. We use Expected Sarsa to learn both the SR and the Q-value function from the intrinsic reward. The behavior policy is generated using a Boltzmann policy over the learned Q function, as it empirically performs better than a greedy policy. We apply simple TD Expected Sarsa updates instead of Emphatic TD(λ) as shown in Algo 2 in McLeod et al. (2021). The learning rates for SR, reward weights, and behavior policy Q function are kept the same.

(4)`BPS`**:** (Hanna et al., 2017) Use a Reinforce style estimator to learn $IS(\tau,\pi) = G(\tau)\Pi_{t=1}^{T}\frac{\pi(a_t|s_t)}{\mu(a_t|s_t)}$, as mentioned in the original paper. Since, the original work is only about single policy evaluation,

we extended for multiple GVFs by updating behavior policy as summation over $\sum_i IS(\tau, \pi_i)$. The behavior policy weight θ is updated as:

$$\theta_\mu = \theta_\mu + \alpha \sum_{i=1}^{n} IS(\tau, \pi_i)^2 \sum_{t=1}^{T} \nabla_\theta \log \mu_\theta(a_t|s_t).$$

B.2 Types of Cumulants

We consider three different types of cumulants similar to McLeod et al. (2021) as shown in Fig. 5:

- **Constant:** Fixed value cumulant, $c_i^t = c_i$
- **Distractor:** *Stationary cumulant* with reward drawn from normal distribution with fixed mean and variance, $c_i^t = \mathcal{N}(\mu_i, \sigma_i)$
- **Drifter:** *Non-Stationary cumulant* whose value change over time, $c_i^t = c_i^{t-1} + \mathcal{N}(\mu_i, \sigma_i), c_i^0 = 100$.

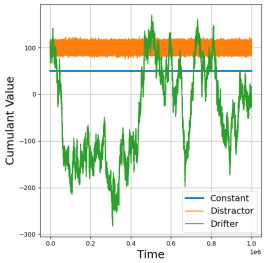

Figure 5: Visual representation of cumulants.

B.3 Tabular Experiments

We consider a tabular 20×20 grid environment with stochastic dynamics. We use the above target policies for the different experimental settings. The Table 1 summarizes the averaged MSE with the same 2×10^6 samples for different experimental settings.

Table 1: **Avg. MSE Summary in Tabular Env:** Compares the average MSE across multiple GVFs in different experimental settings in Tabular environment. We compare baselines with `GVFExplorer` at same 2×10^6 steps of learning. We show the % improvement in `GVFExplorer` w.r.t. to best baseline `RoundRobin`. *Note: Smaller MSE indicates better performance.*

Avg MSE @ $2e6$ steps	`BPS`	`SR`	`UniformPol`	`RoundRobin`	`MixPol`	`GVFExplorer` **(Ours)**	**% Improvement of Ours** (against best baseline)
Distinct policies same cumulant	26.13	2.76	1.22	1.15	1.15	**0.24**	79%
Distinct policies distinct cumulants	8.2	4.1	0.54	0.47	0.44	**0.04**	91%
Non-Stationary cumulants in FR env ($4M$ steps)	18.57	1.78	0.9	1.28	1.08	**0.46**	48%
Large num of GVFs	-	53.3	2.66	2.35	2.64	**1.66**	29%

Table 2: **Optimized Hyperparameters:** We show the optimized hyperparameters for different Experimental Settings. α_Q is learning rate for value function. α_M is learning rate for variance function.

Exp. Settings	**distinct policies identical cumulants**	**distinct policies distinct cumulants**	**large scale 40 GVF eval**	**non-linear func approx**	**non-stationary cumulant in FR**
`GVFExplorer` (Ours)	($\alpha_Q = 0.25$, $\alpha_M = 0.8$)	($\alpha_Q = 0.1$, $\alpha_M = 0.8$)	($\alpha_Q = 0.5$, $\alpha_M = 0.95$)	($\alpha_Q = 5e-3$, $\alpha_M = 5e-3$)	($\alpha_Q = 0.5$, $\alpha_M = 0.8$)
`RoundRobin`	0.95	0.8	0.8	$5e-4$	0.8
`MixturePolicy`	0.95	0.8	0.8	$5e-4$	0.8
`UniformPolicy`	0.95	0.8	0.8	-	0.8
`SR`	0.25	0.5	0.25	$1e-3$	0.8
`BPS`	0.5	0.8	-	-	0.8

Hyperparameter Tuning: In our experiments, we use linearly decaying learning rates that starts with initial value of 1.0 and gradually decreased to an optimized minimum value within $500K$ steps of environmental interactions. We used different learning rates for value and variance function in `GVFExplorer`. The minimum learning rate parameter was swept within $\{0.1, 0.25, 0.5, 0.8, 0.9, 0.95\}$ for both value and variance function. The optimal minimum learning rate was determined based on the one achieving the lowest average Mean Squared Error

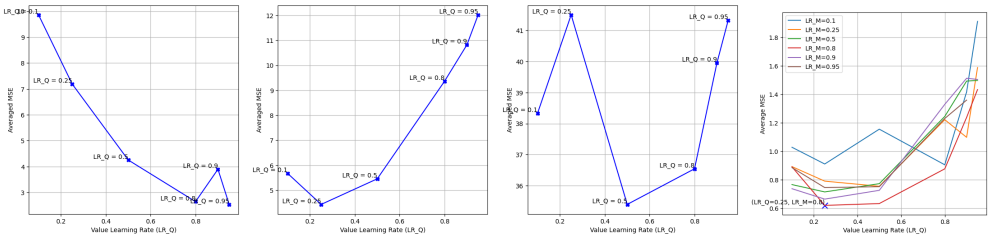

(a) `RoundRobin` (b) `SR` (c) `BPS` (d) `GVFExplorer`

Figure 6: **Impact of Learning Rate on Averaged MSE in Two Distinct Policies & Identical Cumulants scenario**: Demonstrate the effect of changing minimum value of learning rate on the averaged MSE (performance averaged over 10 runs) across GVFs. The optimal hyperparameter is selected based on the least MSE in these plots. LR_Q: value learning rate, LR_M: variance learning rate.

(MSE) after $800K$ sample interactions. **This hyperparameter tuning approach was consistently applied for all algorithms including baselines**. Fig. 6 shows the sensitivity analysis of varying learning rates for value functions (all baselines) and variance functions (our method) with the averaged MSE performance in **Two Distinct Policies & Identical Cumulants**. The learning rate resulting in the lowest MSE was selected as optimal. In Table 2, we show the optimal hyperparameters for the four experimental settings discussed in the paper earlier (refer *Experimental Settings* in Sec. 7).

B.3.1 Two Distinct Policies & Identical Cumulants

In tabular 20×20 grid, we consider distinct target policies with identical distractor cumulant $r = \mathcal{N}(\mu = 100, \sigma = 5)$. In Fig. 7, we depict the individual MSE over 25 runs for both the GVFs $(\pi_1, c), (\pi_2, c)$; showing decreased MSE for `GVFExplorer` compared to the baselines.

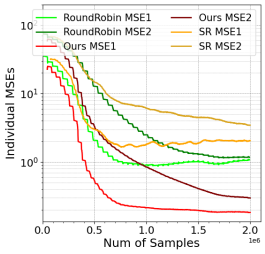

Figure 7: **Two Distinct Policies & Identical Cumulants in 20x20 Grid**: Averaged MSE over 25 runs for two GVFs $(\pi_1, c), (\pi_2, c)$ with same cumulant. We show individual $\text{MSE}_1, \text{MSE}_2$. `GVFExplorer` shows lower MSE compared to other baselines.

B.3.2 Two Distinct Policies & Distinct Cumulants

In tabular 20×20 grid, we consider distinct target policies and distinct distractor cumulants $c_1 = \mathcal{N}(\mu = 100, \sigma = 5)$ placed at top-left corner and $c_2 = \mathcal{N}(\mu = 50, \sigma = 5)$ placed in top-right corner. Fig. 8 shows the individual MSE for all algorithms and the estimated variance in `GVFExplorer` for both the GVFs.

Semi-greedy π for Two Distinct Policies & Distinct Cumulants: We evaluated semi-greedy target policies with distinct cumulants, (π_1, c_1) and (π_2, c_2) within a 20x20 grid. The target policies are designed with a bias towards top-left and top-right goals respectively,

$$\begin{aligned} \pi_1(s) &= \{L : 0.4, R : 0.1, U : 0.4, D : 0.1\} \forall s \in \mathcal{S} \\ \pi_2(s) &= \{L : 0.1, R : 0.4, U : 0.4, D : 0.1\} \forall s \in \mathcal{S}. \end{aligned} \tag{15}$$

We keep the same cumulants same as in previous experiment. Fig. 9 compares the average MSE performance, where `GVFExplorer` exhibits comparable MSE to `RoundRobin` baseline but requires

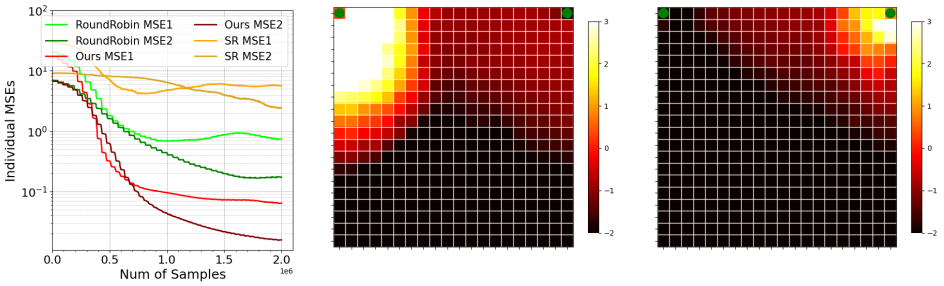

(a) MSE for individual GVFs (b) Var GVF_1(`GVFExplorer`) (c) Var GVF_2(`GVFExplorer`)

Figure 8: **Two Distinct Policies & Distinct Cumulants in Grid env**: Evaluate two distinct GVFs (π_1, c_1) and (π_2, c_2) averaged over 25 runs. Compared baselines – `RoundRobin`, `MixturePolicy`, `UniformPolicy`, `SR`, `BPS` with `GVFExplorer`. Green dots show GVF goals. (a) Individual MSE_1 for GVF (π_1, c_1), and MSE_2 for GVF (π_2, c_2). (b,c) Estimated variance $\hat{M}_{\pi_1}^{c_1}, \hat{M}_{\pi_2}^{c_2}$ in `GVFExplorer`. Variance plots show log-scale empirical values; most areas appear black, due to their relatively small magnitude compared to high variance regions. *The color bar uses log scale & vibrant colors indicate higher values.*

more samples to converge. This outcome can be attributed to the near-greedy nature of the target policies, which inherently guides `RoundRobin` along goal directed trajectories, enabling it to achieve nearly accurate predictions with fewer samples. The optimal hyperparameters for `RoundRobin`, `UniformPolicy` and `MixturePolicy` is $\alpha_Q = 0.95$. We used $\alpha_Q = 0.5, \alpha_M = 0.8$ for ours `GVFExplorer`. Another baseline `SR` has $\alpha_Q = 0.8$ and `BPS` as $\alpha_Q = 0.9$ as optimal hyperparameters.

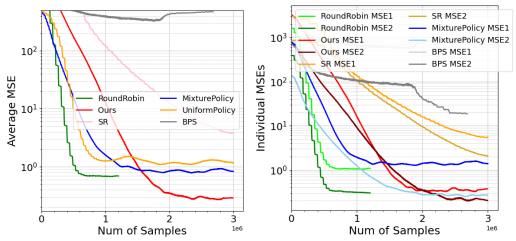

(a) Averaged MSE (b) $\text{MSE}_1, \text{MSE}_2$

Figure 9: **Semi-greedy target policies in Two Distinct Policies & Distinct Cumulants**: Analysis of MSE averaged over 25 runs with semi-greedy target policies. (a) Averaged MSE (b) $\text{MSE}_1, \text{MSE}_2$. We observe a slower convergence of `GVFExplorer` as compared to baselines like `RoundRobin`, `MixturePolicy` due to target policies being semi-greedy.

B.3.3 Ablation Study on Effect in Performance on using Poor Feature Approximator

In this section, we study the effect of using degraded approximations or feature quality on the performance metrics. We conducted an ablation study in a 20x20 grid with two distinct *distractor* GVFs with cumulants, $c_1 = \mathcal{N}(\mu = 100, \sigma = 5)$ placed on the top-left corner and $c_2 = \mathcal{N}(\mu = 50, \sigma = 5)$ on the top-right corner. We reduced the state space into 10x20 and 5x20 feature grids (grouping factors of 2 and 4, respectively), and compared results against the original setup (no approximation, factor = 1). As shown in Fig. 10, the MSE increases as the feature quality deteriorates. Despite this, `GVFExplorer` outperforms `RoundRobin` and `MixturePolicy`, though with very poor approximations (factor = 4), the `UniformPolicy` performs better due to inaccurate variance estimates. These results demonstrate that `GVFExplorer` is robust with moderately coarse approximations but can degrade with significantly poor feature representations, as expected. Further, these results are strengthened by the performance of `GVFExplorer` in Mujoco environments Sec. 7.3.

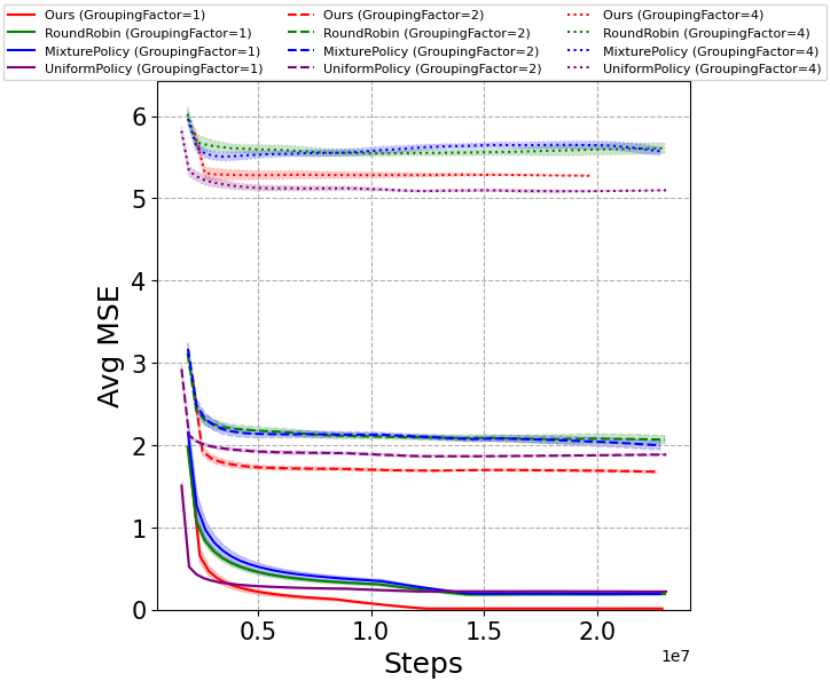

Figure 10: **Impact of Feature Approximation on MSE:** Averaged MSE over 10 runs with standard error in tabular environment. Increasing *GroupingFactor* indicates coarser feature mapping (more states mapped to the same feature). As expected, overall MSE increases with coarser mapping. `GVFExplorer` outperforms baselines given a reasonable feature approximator.

B.3.4 Non-Stationary Cumulant in FourRooms

In complex FourRooms environment, we consider two distinct target policies in App. B.3.5 and different cumulants – stationary **distractor** with $\mathcal{N}(\mu = 100, \sigma = 2)$ in top-left room, non-stationary **drifter** signal of $\sigma = 0.5$ in top-right room. Figs. 11a and 11b shows the change in estimated variance M of `GVFExplorer` from early learning steps to later steps (vibrant color shows higher numerical value). We experimented with changing the value of σ of drifter cumulant to see the effect on MSE. In Fig. 11c we observe that MSE increases with increasing the value of driftness (σ) over time.

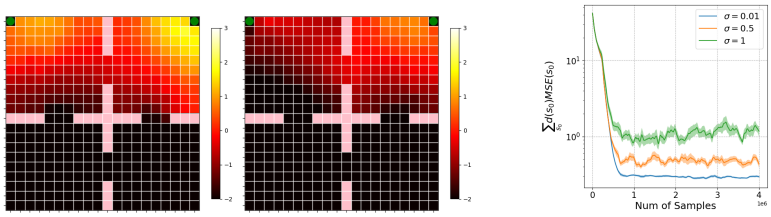

(a) Avg M in early learning stage (b) Avg M in later learning state (c) Avg MSE with different σ of drifter cumulant

Figure 11: **Non-Stationary Cumulant in FourRooms**: We placed a stationary distractor cumulant in the top-left room and a non-stationary drifter cumulant in the top-right room. (a & b) show the change in estimated variance $\hat{M}$ over time, highlighting the effectiveness of `GVFExplorer` in tracking the non-stationary cumulant placed in top-right corner, later in learning process over stationary cumulant (top-left). (c) shows the average MSE for `GVFExplorer` with different levels of driftness (σ) in the cumulant value; higher driftness leads to higher MSE.

B.3.5 Large Scale Evaluation with 40 Distinct GVFs

We evaluate `GVFExplorer` ability to handle a large number of GVFs. We examine four target policies ($\pi_{n\in 1\dots 4}$), each aligned with a cardinal direction, and ten cumulants ($c_{m\in 1\dots 10}$), aiming to predict 40 GVF combinations ($v^{c_1}_{\pi_{1\dots 4}} \dots v^{c_{10}}_{\pi_{1\dots 4}}$). Each GVF is associated with a state space region ("goal"), uniformly sampled and assigned **constant** cumulant value ranging $[50, 100]$, demonstrated in Fig. 12. In this setting, we considered 4 target policies in the four cardinal directions, namely:

$$\pi_N(s) = \{L : 0.1, R : 0.1, U : 0.7, D : 0.1\} \forall s \in \mathcal{S}$$
$$\pi_E(s) = \{L : 0.1, R : 0.7, U : 0.1, D : 0.1\} \forall s \in \mathcal{S}$$
$$\pi_S(s) = \{L : 0.1, R : 0.1, U : 0.1, D : 0.7\} \forall s \in \mathcal{S}$$
$$\pi_W(s) = \{L : 0.7, R : 0.1, U : 0.1, D : 0.1\} \forall s \in \mathcal{S}.$$

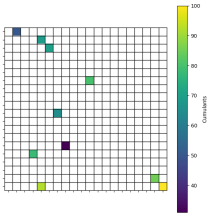

Figure 12: 10 different cumulants for **Large Scale Evaluation with 40 Distinct GVFs** in 20×20 grid. The color depict the cumulant empirical value.

B.3.6 Ablation: IS ratios vs Expected Sarsa Update

In FourRooms environment with distractor and drifter cumulants (two distinct GVFs), we compare the following off-policy update styles: (1) Off-policy TD updates using IS ρ correction,

$$Q(s_t, a_t) = Q(s_t, a_t) + \alpha_Q(\underbrace{c_t + \gamma\rho_{t+1}Q(s_{t+1}, a_{t+1}) - Q(s_t, a_t)}_{=\delta_Q})$$

$$M(s_t, a_t) = M(s_t, a_t) + \alpha_M(\delta_Q^2 + \gamma^2\rho_{t+1}^2 M(s_{t+1}, a_{t+1}) - M(s_t, a_t)$$

and (2) Expected Sarsa update in Eqs. (5) and (6). In Fig. 13, we observe that Expected Sarsa leads to lower MSE, hence we use Expected Sarsa for all the TD updates in *all the algorithms* including baseline for further update stability.

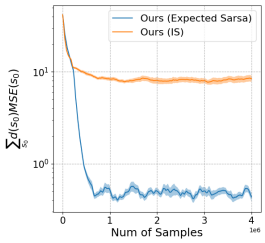

Figure 13: **IS vs Expected Sarsa update in FR env:** We show the averaged MSE (over 25 runs) in Fourrooms by doing off-policy IS corrections in TD updates and off-policy Expected Sarsa in `GVFExplorer` algorithm. Expected Sarsa leads to smaller MSE and faster convergence.

B.4 Continuous State Environment with Non-linear Function Approximation

Continuous Environment. We extend the tabular GridWorld environment to a continuous state space, similar to the approach by McLeod et al. (2021). The environment is a square of dimension 1×1 with four discrete actions. We evaluate two GVFs: the first GVF has a cumulant at the top-left corner, $c_1 = \mathcal{N}(\mu = 100, \sigma = 5)$, and the second at the top-right corner, $c_2 = \mathcal{N}(\mu = 50, \sigma = 5)$. The target policies are consistent with those used in the tabular environment. The agent receives a

zero cumulant signal elsewhere and moves 0.025 units in the selected direction with added uniform noise $\mathcal{U}[-0.01, 0.01]$. Episodes start randomly, excluding a 0.05 radius from the goal state, and end after 500 steps or upon reaching a 0.05 radius from the goal.

Fig. 14 presents the individual MSE for both GVFs under standard Experience Replay and PER. Our method, `GVFExplorer`, consistently achieves lower MSE compared to baselines. Fig. 15 shows the absolute GVF value prediction error with PER for both the baseline `RoundRobin` and `GVFExplorer`. Fig. 16 illustrates the estimated variance from each GVF, underscoring the necessity for a sampling strategy that prioritizes high-variance return areas to reduce data interactions and ultimately reducing the variance and MSE. Fig. 17 depicts the trajectories sampled from baseline `RoundRobin` and `GVFExplorer`. Table 3 summarizes the performance of various algorithms in this continuous environment.

Computation of True GVF Values. The true GVF values in a continuous environment are computed using a Monte Carlo (MC) method. The continuous state space is discretized into a grid, with an initial state sampled from each grid cell. We calculate the average discounted return over $200,000$ trajectories following policy π_i with cumulant c_i. The mean squared error (MSE) between the estimated and true GVF values is then computed using these discretized states, expressed as $\mathbb{E}_i\left[\sum_s \left(V_{\pi_i}^{c_i}(s) - \hat{V}_{\pi_i}^{c_i}(s)\right)^2\right]$ for all algorithms.

Network Architecture. We use distinct deep networks for learning value Q and variance M. Both networks share a similar architecture, with a shared feature extractor for input states and separate output heads for each GVF, producing multidimensional outputs for both value and variance. The variance network includes a Softplus layer before each head's output to ensure positive numerical values.

Table 3: **Avg. MSE Summary for Continuous Env.**: Averaged MSE across two GVFs for different algorithms in the continuous environment. `GVFExplorer` performance measured against others using **standard** and **prioritized experience replay** after 1×10^6 learning steps. *Note: Smaller MSE indicates better performance.*

Avg MSE @$1e6$ steps	`SR`	`MixturePolicy`	`RoundRobin`	`GVFExplorer` (Ours)	**% Improvement of `GVFExplorer` (against best baseline)**
Standard Replay Buffer	21.7	18.25	16.78	**5.19**	69%
Prioritized Exp. Replay	112	14.7	11.62	**3.87**	66%

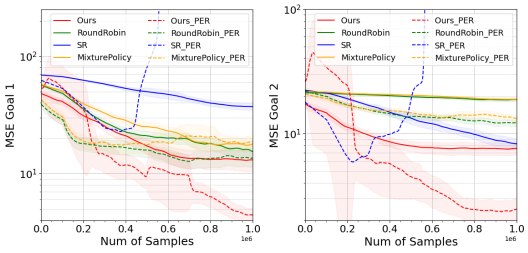

(a) MSE Left Goal (b) MSE Right Goal

Figure 14: **Individual MSE in Continuous Env.**: Compare the MSE metrics in baselines - `RoundRobin`, `MixturePolicy`, `SR` and `GVFExplorer` (averaged over 50 runs with standard errors) for both standard **Experience Replay Buffer** (solid lines) and with **Priority Experience Replay** (PER) (dotted lines). `GVFExplorer` demonstrates lower MSE with both types of replay buffers. PER generally reduces MSE across all algorithms, except for `SR`.

B.5 Mujoco Environment with Continuous State-Action Tasks

We conducted additional experiments using the DM-Control suite in the Mujoco environment, focusing on the *Walker* and *Cheetah* domains. For the *Walker* domain, we defined two distinct

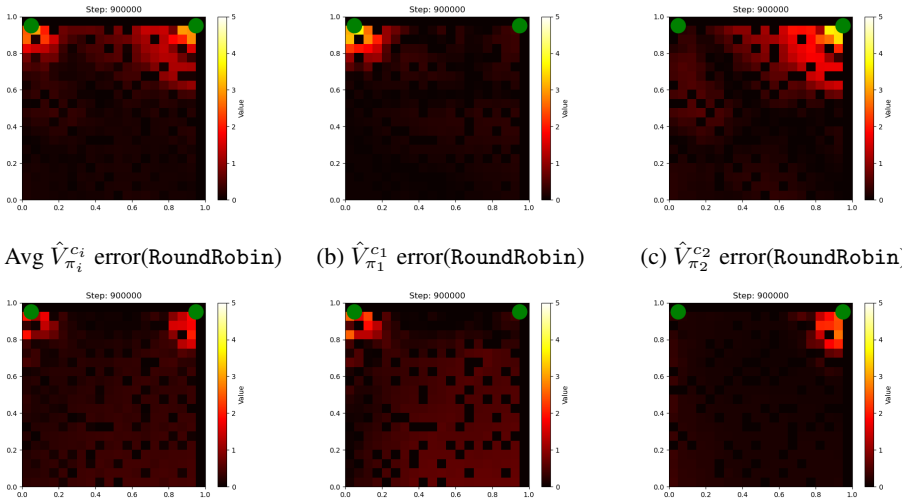

(a) Avg $\hat{V}^{c_i}_{\pi_i}$ error(`RoundRobin`) (b) $\hat{V}^{c_1}_{\pi_1}$ error(`RoundRobin`) (c) $\hat{V}^{c_2}_{\pi_2}$ error(`RoundRobin`)

(d) Avg $\hat{V}^{c_i}_{\pi_i}$ error(`GVFExplorer`) (e) $\hat{V}^{c_1}_{\pi_1}$ error(`GVFExplorer`) (f) $\hat{V}^{c_2}_{\pi_2}$ error(`GVFExplorer`)

Figure 15: **Value Prediction Errors in Continuous Env**: Compares log-scale absolute errors between actual and predicted values for two GVFs. Top row: `RoundRobin` baseline errors; Bottom row: `GVFExplorer` results at equivalent steps. **(Col 1)**: Mean error, **(Col 2)**: Error in GVF 1, **(Col 3)**: Error in GVF 2. `GVFExplorer` specially achieves smaller errors in areas where `RoundRobin` has higher MSE, due to the focus on reducing overall MSE (indicated by lighter colors).

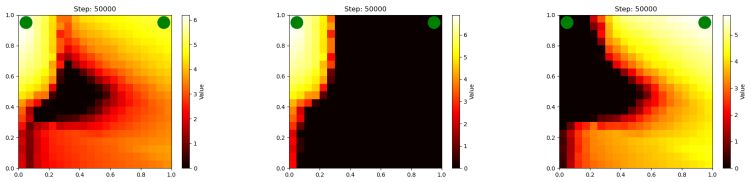

(a) $\mathbb{E}_{i=\{1,2\}}[M^i(s)]$ (b) $M^1(s)$ (c) $M^2(s)$

Figure 16: **Estimated Variance in Continuous Env**: The two GVF goals are depicted in Green. We show the estimated variance M (log values) over states from `GVFExplorer` method highlighting the motivation for behavior policy to visit high variance areas. (a) Mean variance, (b) Variance for left goal GVF, (c) variance for right goal GVF. These variance plots show log scale empirical values; most areas appear black due to their relatively small magnitude compared to high variance regions.

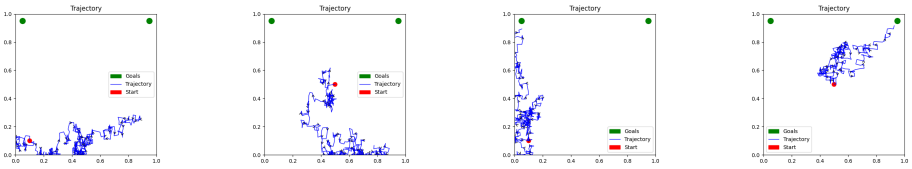

(a) `RoundRobin` τ_1 (b) `RoundRobin` τ_2 (c) `GVFExplorer` τ_1 (d) `GVFExplorer` τ_2

Figure 17: **Sampled trajectories in Continuous Env**: `GVFExplorer` generates trajectories which reduces the overall variance, thus minimizing the total MSE. Contrary, `RoundRobin` collects data according to given target policies. Green dots show GVF goals and red depicts the start state.

GVFs: *walk* and *flip*. In the *Cheetah* domain, we evaluated two GVFs: *walk* and *run*. To handle the continuous action space in these environments, we leveraged policy gradient methods, which are essential when working with continuous actions, as value-based methods like Q-learning are not directly applicable.

Our method can be incorporated with any policy gradient (PG) algorithm. For these experiments, we used Soft Actor-Critic (SAC)(Haarnoja et al., 2018) which provides stability in such settings. SAC uses an entropy regularizer to encourage **exploration**, where the regularization coefficient α is learned adaptively. This allows the agent to balance exploration and exploitation effectively. We present the SAC-based `GVFExplorer` in Algorithm 2 below.

We introduced a separate variance network to estimate the variance of the return (M critic). The behavior policy interacts with the environment, collects samples, and updates the Q-value and M-variance networks. The policy is then updated to minimize the mean squared error (MSE) objective by minimizing the variance. To ensure that the behavior policy does not diverge from the target GVF policies, we added a KL regularizer between the behavior policy and the target policies associated with each GVF.

To calculate the MSE between the true GVF values and the outputs of the Q-critic network, we need accurate estimates of the true Q-value function. Since obtaining the exact Q-values is infeasible, we approximated using Monte Carlo (MC) methods. We rolled out 100 episodes to estimate the Q-value $Q(s, a)$ for a fixed set of sampled states. We chose a set of 50 states from the environment to perform this estimation. The MSE was then computed by comparing the Q-values produced by the learned Q-network to these MC estimates.

We used TD3 to train target policies for each GVF and selected mid-level performing policies. This setup allows the behavior policy to efficiently gather data for parallel GVF estimation.

In summary, `GVFExplorer` scales to continuous action domains using SAC with entropy-based exploration, and it effectively estimates GVFs in Mujoco environments. Fig. 4 shows that `GVFExplorer` lowers MSE more effectively than baselines `RoundRobin` and `UniformPolicy`.

Algorithm 2: SAC-based `GVFExplorer`

Input: Target policies $\pi_{i\in\{1,\ldots,n\}}$, initialized behavior policy μ_ϕ, replay buffer $\mathcal{D}$, primary networks Q with θ_1, θ_2, primary M variance with w_1, w_2, target networks $Q_{\bar{\theta}_1}, Q_{\bar{\theta}_2}$, $M_{\bar{w}_1}, M_{\bar{w}_2}$, learning rates α_Q, α_M, mini-batch size b, entropy coefficient α, update frequencies p, m, l, target entropy $\bar{H}$, training steps K

for *environment step* $k = 1, \ldots, K$ **do**
  Select action $a \sim \mu_\phi(\cdot|s)$
  Observe next state s' and cumulants c
  Store transition (s, a, s', c) in replay buffer $\mathcal{D}$
  if $step\%p == 0$ **then**
    Sample mini-batch $\mathcal{D} \sim (s, a, s', c)$
    //Q-critic update
    Compute $Q_{tar}(s,a) = c + \gamma\left(\min_{d=1,2} Q_{\bar{\theta}_d}(s', a' \sim \pi_i(\cdot|s')) - \alpha \log \mu_\phi(\bar{a}|s')\right)$, $\bar{a} \sim \mu_\phi(\cdot|s')$
    Update Q_θ with MSE loss: $(Q_{tar} - Q_{\theta_d}(s,a))^2$ for $d = 1, 2$
    //Compute TD error
    $\delta_Q = Q_{tar} - \min_{d=1,2} Q_{\theta_d}(s,a)$
    //Variance-critic update
    Compute $M_{tar}(s,a) = \delta_Q^2 + \gamma^2\left(\min_{d=1,2} M_{\bar{w}_d}(s', a' \sim \pi_i(\cdot|s')) - \alpha \log \mu_\phi(\bar{a}|s')\right)$, $\bar{a} \sim \mu_\phi(\cdot|s')$
    Update M_w with MSE loss: $(M_{tar} - M_{w_d}(s_t, a_t))^2$ for $d = 1, 2$
  end
  if $step\%l == 0$ **then**
    Update target networks: $\bar{\theta}_d = \theta_d$, $\bar{w}_d = w_d$
  end
  if $step\%m == 0$ **then**
    // Update behavior policy μ_ϕ
    Update ϕ using $\nabla_\phi \sum_{s\sim\mathcal{D}} \left(\min_{d=1,2} M_{w_d}(s, \bar{a}) - \alpha \log \mu_\phi(\bar{a}|s)\right)$,
    where $\bar{a}$ is sampled from $\mu_\phi(\cdot|s)$.
    //Update α entropy regularizer
    Update α with loss $(-\alpha \log \mu_\phi(\cdot|s) + \bar{H})$
  end
end
Returns Estimated GVF values $Q_\theta^i(s, \cdot)$ for $i = \{1, \ldots, n\}$